Available online at www.sciencedirect.com

ScienceDirect

journal homepage: www.intl.elsevierhealth.com/journals/dema

Antibacterial resin-based composite containing chlorhexidine for dental applications

Letícia Cristina Cidreira Boaro[a,b,*], *Luiza Mello Campos*[b], *Gustavo Henrique Costa Varca*[b], *Tamiris Martins Ribeiro dos Santos*[b], *Pamela Adeline Marques*[a], *Mari Miura Sugii*[c], *Nathalia Ramaldes Saldanha*[a], *Karina Cogo-Müller*[c], *William Cunha Brandt*[a], *Roberto Ruggiero Braga*[d], *Duclerc F. Parra*[b]

[a] *Universidade Santo Amaro – Faculdade de Odontologia, 04829-900, São Paulo, Brazil*
[b] *Instituto de Pesquisas Energéticas e Nucleares IPEN-CNEN/SP, 05508-000, São Paulo, Brazil*
[c] *Universidade Estadual de Campinas – Faculdade de Odontologia, 13414-903, São Paulo, Brazil*
[d] *Universidade de São Paulo – Faculdade de Odontologia, 05508-000, São Paulo, Brazil*

ARTICLE INFO

Article history:
Received 26 June 2018
Received in revised form
11 March 2019
Accepted 15 March 2019

ABSTRACT

Objeticve. The aim of this study was to develop a composite material with antibacterial activity using MMT loaded with clorhexidine (CHX). For that it was used a BisGMA/TEGDMA matrix and added low concentration of MMT/CHX. The aim was to evaluate the drug release capacity of MMT, and not to provide reinforcement.

Methods. Six experimental composites were made with organic matrix of BisGMA/TEGDMA in equal proportions by weight. The composites received organophlizated montmorillonite with or without CHX. The concentrations were 2,5; 5 or 10% by weight. Degree of conversion (DC) was evaluated using FTIR (peak 6165 cm-1; n = 5). Specimens for flexural properties (10×2×1 mm) were immediate tested (24h). Elastic modulus(E) and flexural strength (FS) was measured using the three point bending test (n = 10). Inibition halo was used to test the antibacterial activity against *Staphylococcus aureus*, *Streptococcus mutans*, and *Porphyromonas gingivalis* (n = 5 for each bacteria). The inhibition of biofilm formation (BF) was evaluated by inserting polymerized disc of composite in to a culture media colonized with *Streptococcus mutans* (n = 10). The release of CHX was measured using ultraviolet (255 nm) for 10 days (n = 5). The data of degree of conversion was analysed using Kruskal–Wallis/ Mann–Whitney, and the other variables using two-way ANOVA/Tukey, always considering a global level of significance of 5%.

Results. DC ranged from 71% to 74%. E ranged from 5.7 to 8.1 GPa. FS ranged from 61.4 to 74.7 MPa. There were no statistical differences among the groups for all the variables. For the three bacteria tested the composites with CHX loaded presented inhibition of growth for all concentration, except for 2,5% that did not inihibited the growth of *P. gingivalis*. BF was lower for the groups with 10% MMT/CHX, all groups presented BF, even those without CHX loaded. All concentrations presented release off CHX during all the 28 days analyzed.

* *Corresponding author at*: Faculdade de Odontologia, Universidade Santo Amaro, Rua Professor Eneas de Siqueira Neto, 340; CEP: 04829-900, São Paulo, SP, Brazil.
E-mail addresses: lboaro@prof.unisa.br, leticiaboaro@usp.br (L.C.C. Boaro).
https://doi.org/10.1016/j.dental.2019.03.004

Conclusions. Within the limitation of this study it can be concluded that: all concentrations tested presented release of CHX and reduced BF. All concentration presented antibacterial activity for the three bacteria tested, except for 2,5% that did not inhibit the growth of *P. gingivalis*. The presence of MMT with CHX loaded did not interfere in the properties evaluated.

1. Introduction

Dimetacrylate-based compositematerials have been used in dentistry for several decades [1]. Even with the huge improvement of those materials, secondary caries remains a problem, representing the main cause of restoration failure [2–5]. On the other hand, in amalgam restorations the interface is sealed by corrosion products such as tin, silver and copper oxides. Silver is a well-known antibacterial agent [6,7] likely to contribute for the low incidence of interfacial caries in amalgam restorations. Unfortunately, the demand for aesthetics as well as environmental concerns regarding the use of mercury are driving silver amalgam into obsolescence. Thus, in order to reduce the risk of secondary caries around composite restorations, the development of tooth-colored materials with antibacterial activity is necessary [3].

The literature presents some interesting alternatives to develop an antibacterial composite, two of them are more frequently reported: (1) composite containing non-releasing antibacterial agents such as monomers modified by quaternary ammonium [8,9]; and (2) composites containing releasing antibacterial agents such as fluorides, silver and chlorhexidine [10,11]. All those alternatives present high effectiveness in killing bacteria in both planktonic and biolfim form, but some studies do not explore the mechanical properties, or report a decrease in those properties.

Chlorhexidine is an organic antibacterial agent widely used in dentistry for the treatment and prevention of bacterial infections which presents low toxicity to soft tissues. It has been considered the gold standard in combating plaque and gingivitis in for the past decades [12]. Even thought is widely used, chlorhexidine may cause mitochondrial injury reducing cell viability [13] and this injury is time and concentration dependent [13,14]. Currently, chlorhexidine is used in low concentration solutions such as for mouthwashes. In order to be released into the tooth/restoration interfacial gap chlorhexidine must be incorporated in the resin-based composite and released through diffusion. One possible strategy is to use a ceramic material as carrier. Montmorillonite (MMT) is a nanoclay used as a pharmaceutical excipient for controlled drug release due to its capacity to absorb organic molecules [12,15–17]. Recently, it was found that the chlorhexidine-loaded MMT (CHX/MMT) presents a significant antibacterial effect. [12] MMT particles may also reinforce polymeric materials such as dimethacrylate-based dental resins [18,19]. Also, the association of MMT/CHX can significantly reduce the chlorhexidine cytotoxicity to human fibroblasts [20].

Thereby, the aim of this study was to develop a composite material with antibacterial activity using CHX/MMT. The CHX/MMT particles were characterized and incorporated into a resin matrix at different filler fractions. The null hypotheses tested were (1) the addition of CHX/MMT does not interfere with the composite mechanical properties and; (2) No increase in composite antibacterial activity.

2. Materials and methods

2.1. CHX/MMT particles

Organophlizated MMT particles (Cloisite 30B, Southern Clay Products, Texas, USA) were dispersed in a 10% chlorhexidine diacetate monohydrate (w/v) aqueous solution using a 10: 1 ratio (w/w). The mixture was kept under constant stirring for 3 hours at 80 °C. The precipitate was filtered, rinsed with water and lyophilized.

The fraction of CHX added into the particles was determined by thermogravimetry analysis. The thermal decomposition profile of MMT particles, CHX and the mixture MMT/CHX were evaluated by thermogravimetry analysis (TGA/SDT851, Mettler Toledo, Berlim, GER) using temperatures ranging from 40 to 800 °C, at the heating rate of 10 °C min^{-1} in dynamic N_2 atmosphere.

The type of interaction between MMT particles and CHX was evaluated by XRD analysis. The interlamellar spacing "d_{001}" characteristic peak for the nanoclay MMT Cloisite® 30B was "d_{001}" = 1.81 nm. XRD diffratograms were obtained using a difractometer (X'Pert PRO with X'Celerator detector PAN analytical brand Rigaku D, Company, Coutry) with Cu Kα radiation (λ = 1.54186 A, 45 kV, 40 A) at room temperature. The diffraction was scanned from 1.17° to 40° in 2θ range with 0.03° step at step/time 100 s. The interlamellar spacing was calculated according to Bragg's equation [21].

$$n\lambda = 2d_{hkl}\sin\theta \quad (1)$$

where n is an integer, λ is the incident wavelength, d is the spacing between the planes of same (hkl) (Miller index) in the crystal lattice, and θ is the angle between the incident ray and the crystal plane.

The particles were also evaluated by scanning electron microscopy (SEM) and the particle size distribution was determined by laser scattering using isopropyl alcohol as dispersant.

2.2. Composite preparation

Six experimental composites were manufactured with the organic phase consisting of BisGMA (Bisphenol A

Bis(2-hydroxy-3-methacryloxypropyl)Ether, Esstech, Essington, Pennsylvania, USA) and TEGDMA (Triethyleneglycol Dimethacrylate, Esstech, Essington, Pennsylvania, USA) in equal proportions by mass. MMT particles, in presence or absence of chlorhexidine were added to the resin to reach concentrations of 2.5, 5 or 10% (w/w). The photoinitiator system consisted of a tertiary amine (DMAEMA (2-(Dimethylamino) ethyl methacrylate), 98%, Sigma-Aldrich Chemie, GmbH, Steinheim, GER) at a concentration of 1% and camphorquinone 0.8% (w/w) (camphorquinone 97%, Sigma-Aldrich Chemie, GmbH, Steinheim, GER).

2.3. Biomaterial characterization

The degree of conversion was determined in a near infrared spectrophotometer with Fourier transform (FT-IR; Vertex 70, Bruker Optik GmbH, Germany) [22]. The specimens (n = 5) were made using a 7.0 mm diameter and 1.0 mm thick between two glass slides silicone mold. After insertion of the composite, the assembly was positioned in the FTIR sample holder and spectra were recorded before and 10 min after photopolymerization using 18 J/cm^2 (720 mW/cm^2 for 25 s; Radii-cal LED light curing, SDI Dental Limited, AUS). The area under the peak 6165 cm^{-1} corresponding to vinyl bond, was calculated. The degree of conversion was calculated considering the spectrum area of the polymerized and uncured material according to the following equation:

$$DC = \left(1 - \frac{Polymerized}{Not\,polymerized}\right) . 100 \quad (2)$$

For each composite, 10 bar-shaped specimens were made using a split steel mold (10 × 2 × 1 mm) [23]. Photoactivation was performed using a radiant exposure of 18 J/cm^2. The specimens were dry stored at 37 °C for 24 h. The three-point bending test was performed using an universal testing machine (Instron 5565, Canton, MA, USA) with 8 mm distance between supports and cross-head speed of 0.5 mm/min. Flexural modulus was calculated according to the following formula:

$$E = \frac{C \times L^3}{4 \times b \times h^3 \times d} \times 10^{-3} \quad (3)$$

where: E is the flexural modulus (GPa), C is the load recorded (N), L is the span between the supports (mm), b is the width of the specimen (mm), h is the height of the specimen (mm) and d is the deflection corresponding to C (mm).

Flexural strength was calculated according to the following formula:

$$\sigma = \frac{3 \times F \times L}{2 \times b \times h^2} \quad (4)$$

where: σ is the flexural strength (MPa), F is the maximum load recorded before the specimen fractured (N), L is the span between the supports (mm), b is the width of the specimen (mm), and h is the height of the specimen (mm).

Composite samples with 60 nm thickness slices were obtained using a ultramicrotome and placed on 200 cooper mesh TEM grids for transmission electron microscopy analysis on a electron microscope (JEOL -JEM 1010, GmbH, GER).

Disc shaped specimens of 5 mm diameter and 1 mm high were made only for the composites with CHX/MMT (n = 5). Specimen photopolimerization was performed as above mentioned. The initial mass of the speciments was registered prior to immersion in 5 mL of 50 mM phosphate buffered saline solution (pH 7) at 37 °C. Aliquots of 200 μl of the upernatant were collected for a 28 days period. Chlorhexidine was quantified by UV spectrophotometry at the wavelength of 255 nm (Spectramax i3x Molecular Devices, California, USA). At the end of the experiment the specimens were re-weighted.

2.4. Antibacterial activity assessment

Antibacterial activity was evaluated by two methods: agar dilution method and biofilm formation. Agar dilution method was chosen to test the antimicrobial effect on planktonic growth while biofilm test was carried out to test whether the composite could inhibit bacterial adhesion and/or biofilm formation. Disc-shaped specimens of 7 mm diameter and 1 mm thickness were made for each composite (n = 15) and photopolimerized as described above.

Porphyromonas gingivalis W83, *Streptococcus mutans* UA159 and *Staphylococcus aureus* ATCC 29213 were tested in the agar dilution method while *S. mutans* UA159 was used for the biofilm test.

P. gingivalis W83 was cultured in Tryptic soy agar (Difco Co., Detroit, MI, USA) supplemented with 0.2% yeast extract (Difco), 7% defibrinated sheep blood (TSYA – tryptic soy yeast agar), 5 μg/mL of hemin (Sigma) and 1 μg/mL of menadione (Sigma) under anaerobic conditions (10% CO_2, 10% H_2 and 80% N_2) at 37 °C. *S. mutans* and *S. aureus* were cultured in Tryptic Soy agar (TSA – Difco), at 5% CO_2 and under aerobic conditions, respectively.

The agar dilution method was conducted according to Clinical Standard Laboratory Institute M2-A8 protocol with some modifications (CLSI, 2003 [24]). For *S. mutans* and *P. gingivalis* a period of 48 h of incubation under anaerobic conditions was used for bacteria growth, while *S. aureus* was incubated for 24 h aerobically. 3 to 4 colonies were picked from 24 to 48 h agar cultures of *P. gingivalis*, *S. mutans* and *S. aureus* and suspended in TSB tubes for preparation of the bacterial inoculum. The inoculum was adjusted to 0.1 by means of optical density at 660 nm (approximately 1 a 2 × 10^8 CFU/mL) on a spectrophotometer. The bacterial suspension was inoculated all over the agar surface using a sterile swab. TSA was used for *S. aureus* and *S. mutans*, while TSYA was used for *P. gingivalis* growth. Discs specimens (five per bacterial species) were positioned over the agar and the plates were incubated under appropriate conditions for 48 h. After this period, inhibition zones were measured using a calliper rule.

The biofilm assay also evaluated was adapted from previously described methods [25,26]. For bacterial inoculum preparation, a culture of *S. mutans* in BHI with 1% glucose was grown for 18 h at 5% CO_2 at 37 °C [27]. From this culture, 1 mL was transferred to a new tube containing 9 mL of BHI with 1% glucose and incubated in CO_2 5% until growth reached 0.7 (660 nm). Twelve microliters of this inoculum were transferred to each well containing 3 mL of BHI with 1% sucrose. Discs were vertically positioned inside each well of the 24-well polystyrene plates. These plates were then incubated at

CO_2 5% and 37 °C. After 24 h the discs were removed from the wells, gently washed two times with sterile NaCl 0.9% aqueous solution and then placed on tubes containing 5 mL of saline solution.

The biofilm was dispersed by vortexing for 1 min followed by sonication with 5% amplitude and 6 pulses (9.9 s each pulse and a 5-s interval) on a Vibra Cell 400 w (Sonics and Materials Inc, Newtown, CT, USA). Biofilm suspensions were plated on BHI agar and incubated at 37 °C during 48 h in microaerophilic condition. After the incubation period the colony-forming units were quantified.

2.5. *Statistical analyses*

Degree of conversion was analyzed using Kruskall–Wallis/Mann–Whitney tests. Flexural modulus, flexural strength, CHX release, biofilm and agar dilution methods were evaluated by ANOVA/Tukey test. For all tests, the significance level of 5% was considered.

3. Results

3.1. *Thermogravimetry analysis (TGA)*

Fig. 1 showed the decomposition profile of MMT nanoparticle, CHX and CHX/MMT mixture. MMT nanoparticle showed three mass loss events, first event occurred in the range between 50 °C and 120 °C, second event ranging between 280 °C and 390 °C and third event observed between 500 °C and 670 °C. CHX also showed three mass loss events, but at different temperature ranges, the first between 50 °C and 200 °C, second event between 200 °C and 275 °C, and the third between 275 °C and 500 °C.

The MMT/CHX degradation curve presented two mass loss events. The first event occurred between 200 °C and 340 °C and was attributed to the decomposition of CHX absorbed and/or intercalated in the interlayer spaces of the organoclay. The second event occurred in the range of 340 °C to 495 °C possibily due to the degradation of organic phase present in MMT particles and CHX. The MMT/CHX started the mass loss in a lower range of temperature than the MMT pure. Considering the total mass loss, from 0 to 800 °C, it can be observed that MMT/CHX presented a mass loss around 7% higher, when compared to MMT itself.

3.2. *X-Ray diffraction (XDR)*

XRD pattern of MMT particles, CHX and MMT/CHX particles, are shown in Fig. 2. The interlamellar spacing of the "pure" MMT particles was calculated as d_{001} = 1.81 nm, while the "d" values for the MMT/CHX was d = 3.9 nm, suggesting the incorporation of CHX between the MMT layers. Adittionally the interlamellar space of the MMT/CHX incorporated to the composite showed a similar value from the MMT/CHX indicating that MMT particles suffered intercalation/exfoliation while another part remained aggregated, which explains the peaks attributed to "d" at around 3.85 nm.

TEM images are presented in Fig. 4. CHX did not affect the intercalation of the organic matrix into the nanoparticle. SEM images are shown in Fig. 3. The particles presented the same pattern in both cases (with or without CHX), but when CHX is present the particles are smaller than MMT pure. The particle size distribution for MMT pure was d(0.5) = 11.946 μm, and for MMT/CHX d(0.5) = 8.137 μm.

3.3. *Biomaterial characterization*

Table 1 presents the data from degree of conversion (%), flexural modulus (GPa) and flexural strength (MPa). Degree of conversion ranged from 71% to 74%. The flexural modulus ranged from 5.7 to 8.1 GPa. Flexural strength ranged from 61.4 to 74.7 MPa. There were no statistical differences among the groups for all the variables evaluated.

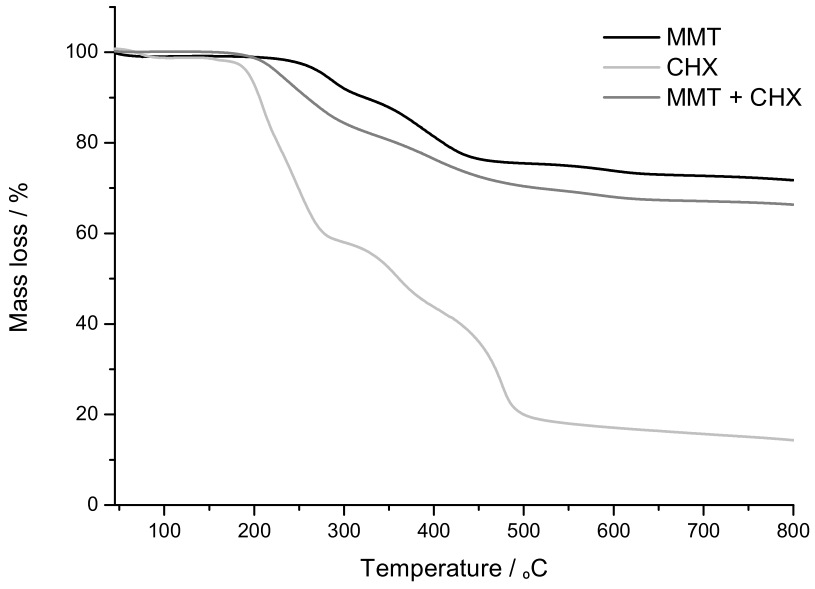

Fig. 1 – Representatives thermograms for MMT+CHX (10:1) compared with the single components.

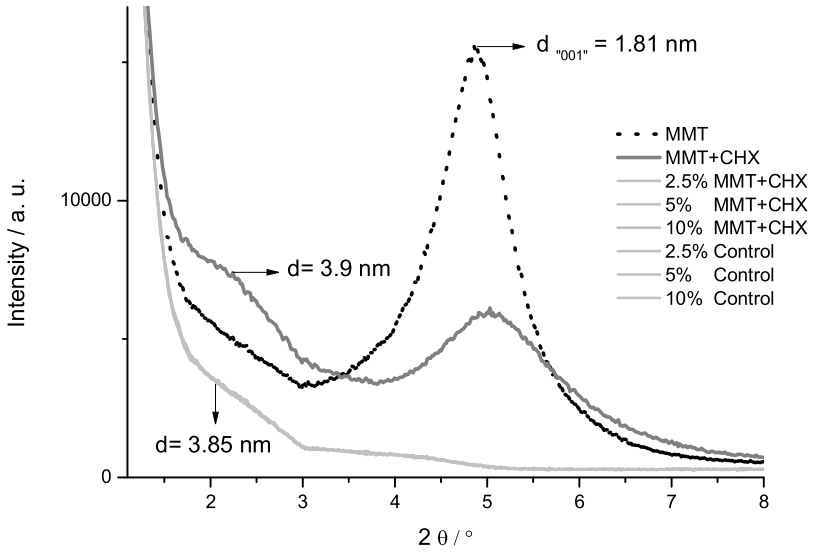

Fig. 2 – XDR analyses of the specimens. The dotted line represents only the MMT. The dark grey line represents MMT with CHX added. The light grey line represents all the groups with polymeric matrix. All the groups with polymeric matrix are overlapped.

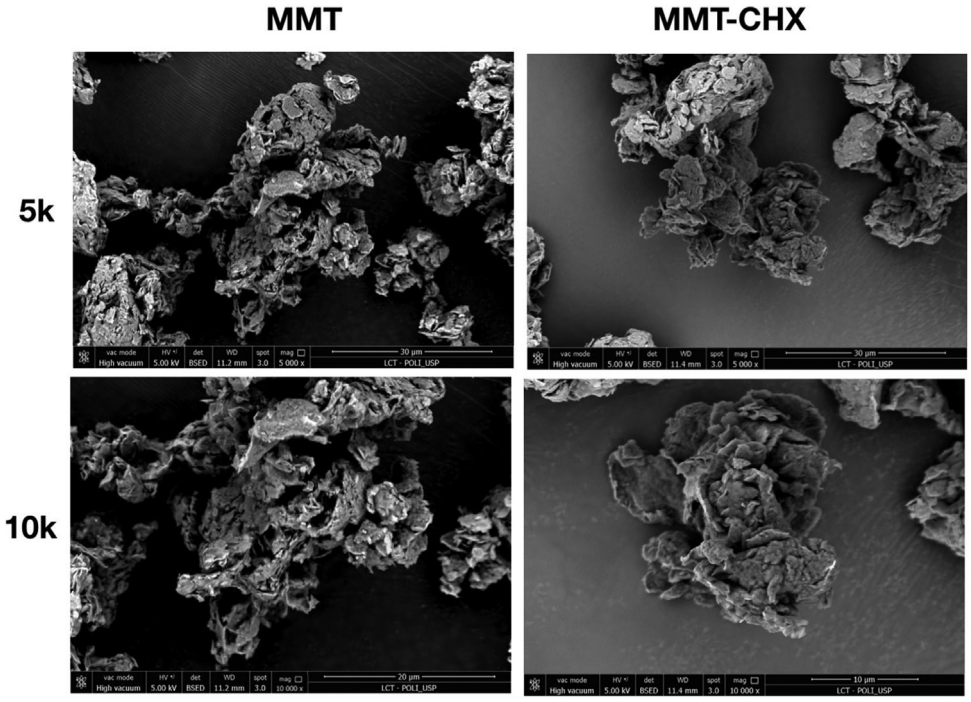

Fig. 3 – SEM micrographs of the nanoparticles with and without CHX at two different magnifications assayed 5000× and 10000×.

3.4. *CHX release*

CHX release is presented in Fig. 5. This graph contains both concentration (mg/mL) of CHX present in the solution in the moment of measurement and the release in percentage considering the initial quantity of CHX present in the specimen. It was possible to observe that the composite containing 2.5% MMT/CHX presented a higher chlorhexidine release of about 45% its initial content over time if compared to the 5 or 10% MMT/CHX in which the CHX release corresponded to about 10–15% during the experiment period. At 5 and 10% MMT/CHX an irrelevant difference in terms of chlorhexidine release was observed. It is important to note that the specimens remained immersed in the same solution during the 28 days of the experiment, making possible to calculate how much of CHX was released based on its initial concentration.

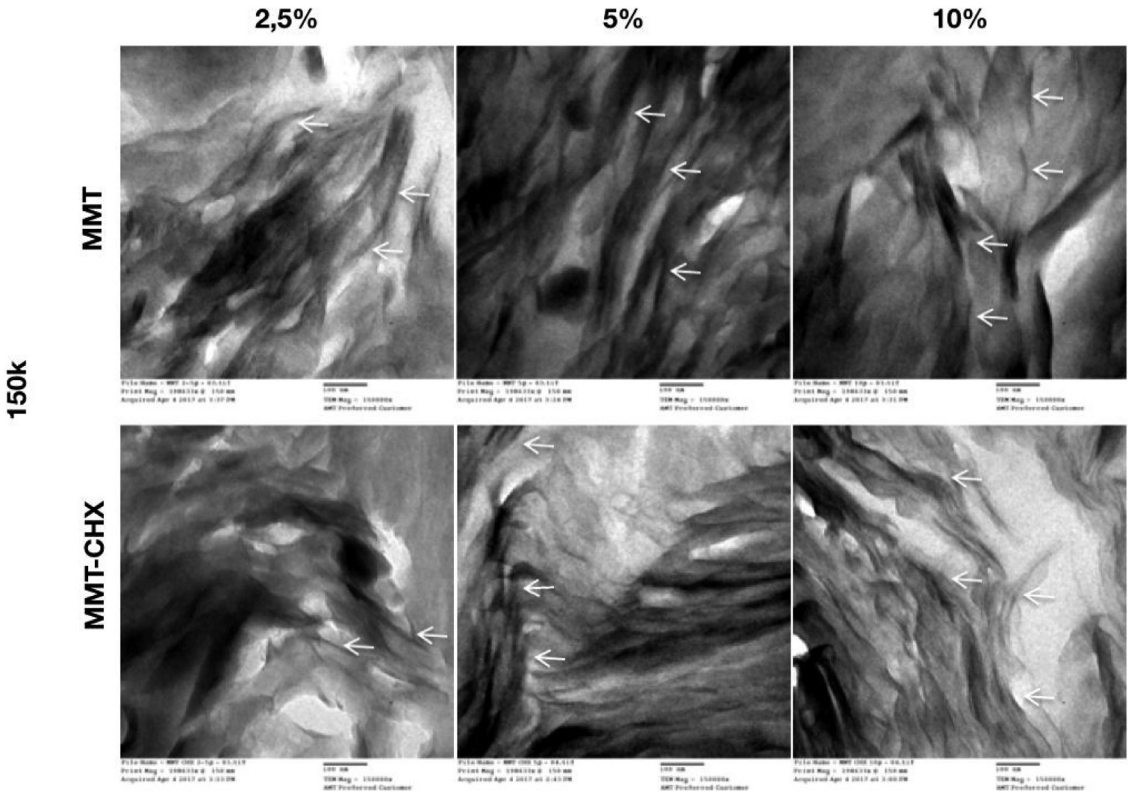

Fig. 4 – TEM micrographs at 150000× magnification of the specimens. Arrows indicate the intercalation of MMT or compound MMT-CHX with the polymeric matrix-based BisGMA/TEGDMA.

Table 1 – Means and standard deviations for elastic modulus (GPa) and flexural strength (MPa) values obtained 24 h after photopolymerization (n = 10), and for degree of conversion 10 min after polymerization (n = 5). There were no statistically difference among all groups (p > 0.05).

MMT % (m/v)	CHX	Elastic modulus (GPa)	Flexural Strength (MPa)	Degree of conversion (%)
Resin matrix		8.1 (1.76)	66.4 (15.5)	74 (7)
2.5	No	7.5 (1.55)	61.4 (15.0)	71 (5)
	Yes	7.1 (1.62)	71.0 (17.6)	74 (8)
5.0	No	7.6 (2.04)	61.9 (17.8)	73 (7)
	Yes	6.4 (1.23)	62.1 (8.8)	74 (3)
10.0	No	5.7 (1.28)	74.7 (17.4)	71 (5)
	Yes	6.9 (2.00)	69.9 (10.0)	72 (6)

3.5. *Antibacterial activity assessment*

Antimicrobial activity of the composites was tested through agar dilution method against strains of *P. gingivalis*, *S. mutans* and *S. aureus*. Results are shown in Fig. 6. For *S. mutans* and *S. aureus*, all experimental groups formed inhibition zones. For *P. gingivalis*, only CHX5 and CHX10 groups presented antimicrobial activity. In general, groups containing chlorhexidine (CHX) promoted higher inhibition compared to MMT groups ($p < 0.05$, ANOVA, Tukey).

For the biofilm formation, no difference was found between MMT and MMT/CHX groups when comparing the same concentrations ($p < 0.05\%$). However, when comparing among CHX groups, CHX10 promoted the highest inhibition ($p < 0,05\%$). There was no statistical difference among the unfilled resin and the groups added with MMT (with or without CHX) for the 2.5 and 5%. In Fig. 7, these data are represented as number of colony forming units per mL (CFU/mL).

4. Discussion

By comparing the thermal decomposition profile of the CHX and the profile of compound MMT/CHX, a delay in the first mass loss event of compound MMT + CHX was observed and these results indicated that the intercalation of CHX between the lamellae of the MMT nanoparticle could improve the thermal stability of CHX corroborating previous studies [12]. The addition of an organic compound such as CHX may be responsible for that behavior. Besides that, this result suggests that the residual of CHX were kept among the nanoparticle layers, which mays justify that the mass loss did not achieve 10% higher than the MMT, corresponding to the initial proportion of CHX added to the MMT.

Fig. 1 reveals that the combination of MMT/CHX presents a distinct profile if compared to the standards alone, which experimentally supported and evidenced the formation of a chemically linked matrix between the components rather than physical interactions alone.

Considering the X-ray diffraction for all experimental groups it was observed that the particles presented intercalation or exfoliation. This can be assumed by the increase of

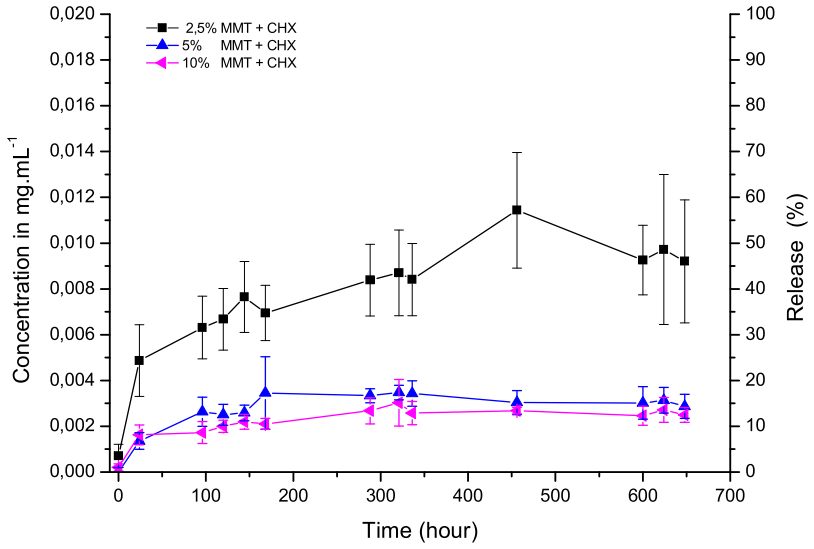

Fig. 5 – CHX release from the developed nanocomposites by means of concentration (in mg/mL) and porcentage (%) as a function of time.

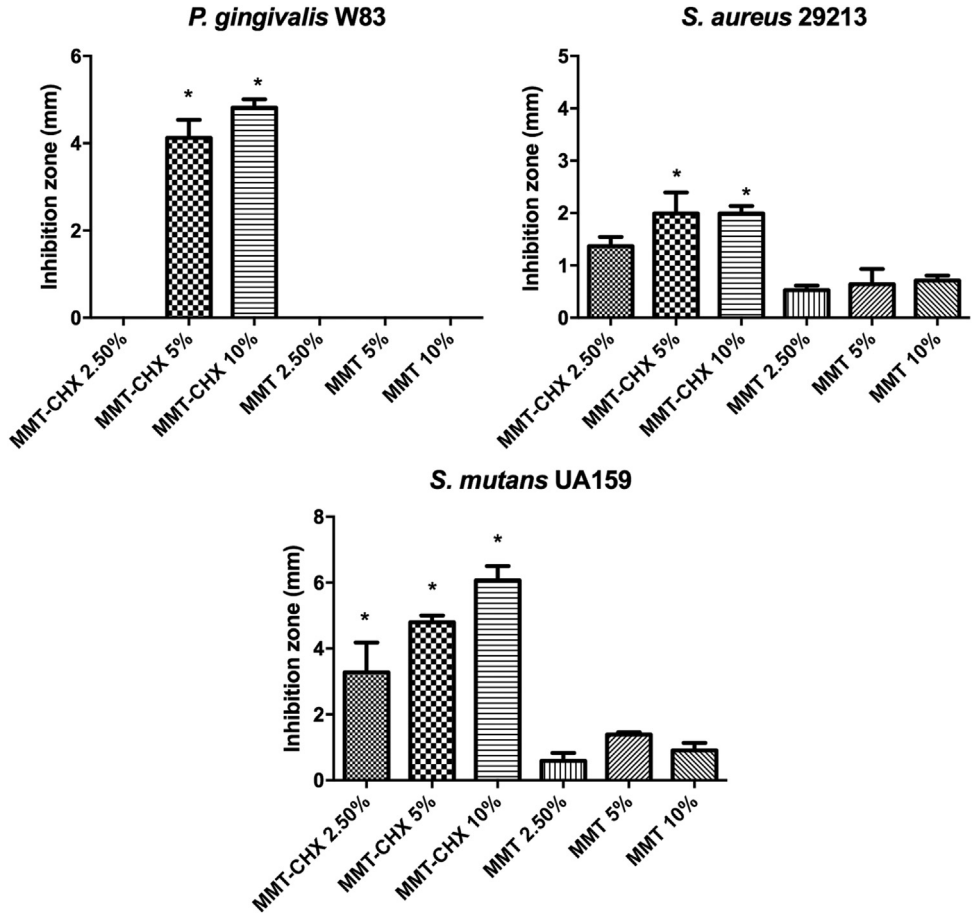

Fig. 6 – Mean values of inhibition zones (mm) calculated representing the antimicrobial activity of CHX and control (CT) nanocomposites. *Represents the statistically relevant differences among CHX and its respective CT group ($p < 0.05$. ANOVA. Tukey).

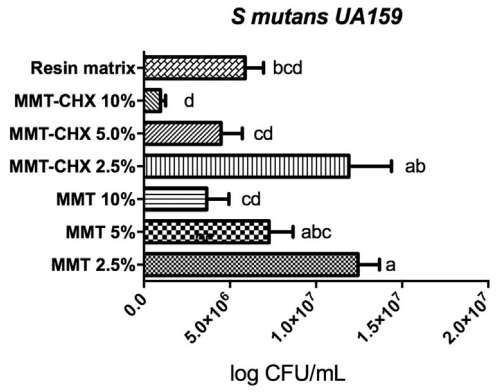

Fig. 7 – Means and standard deviation values calculated for the biofilm formation. Means followed by the same letter were statistically similar ($p < 0.05$).

the basal spacing from 1.81 (MMT pure) to 3,85 for MMT with polymeric matrix, despite the presence of the CHX. This finding is usual when low concentrations of MMT are used [28]. TEM analyses contributed to the X-ray analyses and showed the intercalation for all concentrations used in the present study. In both analyses TEM and SEM the presence of CHX did not affect the distribution of the particles. Regardless the presence of CHX, when the filler content increased the surface were stiffer. No agglomeration of the nanoparticle was observed, usually named tactoid, [29]. The homogeneous surface observed suggest that the nanoparticle even with the presence of CHX are equally distributed into the polymeric matrix.

The particle size distribution and also de SEM of the particles evidence that the CHX resulted in smaller particles, probably due to the exfoliation of the particles caused by the incorporation of CHX into the lamellar configuration of MMT.

BisGMA/TEGDMA is a conventional polymeric matrix used in dentistry, thereby it was chosen to the present study. The low concentration of CHX/MMT tested has the aim to evaluate the drug release capacity of MMT rather than providing reinforcement to the matrix. The first null hypothesis that the addition of chlorhexidine did not interfere in the composite properties was partially accepted. There were no statistically difference among the groups for flexural properties and degree of conversion.

The absence in statistical difference using different filler fraction was expected, but this finding was not expected for flexural properties. Probably this finding can be explained by the low concentration of MMT, as mentioned before, was used as drug delivery vehicle and not as reinforcement of the resin matrix.

The use of UV/visible absorption spectroscopy is widely used to measure CHX release [30–33]. The group with 2.5% of MMT/CHX presented an initial release of CHX, resulting in almost 45% of the initial amount released after 28 days. The other two groups presented a similar slower release, resulting in around 15% of the initial amount released. Even that no statistically difference was observed for the immediate mechanical properties, probably after aging the composite with lower MMT concentration were more susceptible to hydrolytic degradation. Considering the group with 2.5% of MMT/CHX, the burst observed evidences the presence of CHX in the surface of the nanocomposite, especially for the 2.5% MMT/CHX. As the CHX-MMT concentration increased the release profile indicates that less molecules are present in the surface, as revealed by the considerably lower burst observed for these samples, evidencing that the CHX is incorporated into the matrix.

The concentration used of chlorhexidine solutions in dentistry vary from 0.12 to 2% (20 mg/mL to 1.2 mg/mL) [34]. In the present study, nanocomposites released from 0.002 to 0.010 mg/Ml of CHX (0.0002% to 0.001%) at each time evaluated, maintaining a constant release profile. This constant release would be interesting for dental materials applications, as these CHX concentrations could reduce bacterial growth and biofilm formation of micro-organisms in direct contact with the composite, without affecting drastically the composition of the oral microbiota. Thus, the release at low concentrations in a constant pattern could affect less the microbial balance and oral cell's viability, however promoting antimicrobial effect. Concentrations under 0.02% of CHX were much less toxic to fibroblast and osteoblasts than concentrations up to 2%; and in the present study up to 0.001% of CHX was released from composites [14].

The second null hypothesis that the addition of chlorhexidine did not result in the antibacterial activity was partially rejected. The antibacterial activity was dependent on the concentration of complex MMT/CHX added and also on the bacteria species. Regarding the inhibition zone, composites containing chlorhexidine showed better antimicrobial activity than nanocomposites without CHX, suggesting that CHX was released from the composite to the agar medium to promote an inhibition zone around the discs. *S. mutans* and *P. gingivalis* were more sensitive to CHX than S. aureus. but CT groups also formed inhibition zones. However, at 5 % and 10% MMT/CHX, the effect observed is more likely to occur via contact effect rather than by the release of the CHX. This is particularly interesting as less antibiotic is released to the blood to reach the same effect as conventional pharmaceutical forms for the delivery of chlorhexidine.

Biofilm inhibition data showed that only 10% of MM/CHX presented a lower *S. mutans* biofilm formation than the resin matrix itself. Experimental composites have less fillers in their composition making them more susceptible to hydrolytic degradation of the polymeric matrix [35] and, consequently, to the releasing of free monomers [36].

S. mutans is a Gram positive cocci, an important species involved in the formation of cariogenic biofilms when dietary sucrose and starch are present [37–39]. Porphyromonas gingivalis, a Gram negative bacilli, is the major etiologic agent which participates in the development and establishment of periodontitis [40–42]. *S aureus*, also a Gram positive cocci, is an opportunistic and transitory pathogen that can be found in the oral cavity, mainly in peri-implant infections [43]. Therefore, the antimicrobial activity of the nanocomposite suggests a wide range spectrum against oral species; which could prevent bacterial colonization around its surface.

It is established in the literature that long carbon chains may penetrate bacterial membrane causing leakage and death

[44–46]. within this context it is possible to assume that the leachable residual monomers were responsible for the low biofilm formation in the surface observed only when the polymeric matrix was assayed alone. Regarding control groups (without CHX) it was observed a tendency towards a higher biofilm formation in materials with less filler loading.

The MMT nanoparticle (Cloisite 30B) used in this study Holds ammonium quaternary salt in its composition [47], exerting antimicrobial effects [48]. According to the Rhim et al. [50] and Sothornvit et al. [49] the ammonium quaternary salt present in the silicate layer of the nanoparticle is responsible for the break of the bacteria cellular membrane [49,50]. for the MMT/CHX specimens we hypothesize that residual monomers, ammonium quaternary salt and chlorhexidine together were responsible for antimicrobial properties of their composites.

For all mass ratios used CHX was released from the MMT nanoparticle, resulting in a release over time. For the 2.5% of MMT/CHX the release was faster than the others. In the present report, the association between MMT/CHX for dental composites is a promising nanotechnology application in the seek for better alternatives to prevent oral bacterial infections, mainly secondary caries, and also reducing the composite biofilm formation.

In conclusion, MMT/CHX can be used to formulate a resin-based composite with local antibacterial activity against *S. mutans*, *P. gingivalis* and *S. Aureus*, reducing the biofilm formation, without compromising the mechanical properties.

Acknowledgements

The authors would like to thank FAPESP (Project Number 2014/23144-0 and 2016/01319-9). The funders had no role in study design, data collection and analysis, decision to publish, or preparation of the manuscript.

REFERENCES

[1] Bowen RL. Use of epoxy resins in restorative materials. J Dent Res 1956;35(3):360–9.
[2] Boaro LC, et al. Sorption, solubility, shrinkage and mechanical properties of “low-shrinkage” commercial resin composites. Dent Mater 2013;29(4):398–404.
[3] Bernardo M, et al. Survival and reasons for failure of amalgam versus composite posterior restorations placed in a randomized clinical trial. J Am Dent Assoc 2007;138(6):775–83.
[4] Dickinson GL, Gerbo LR, Leinfelder KF. Clinical evaluation of a highly wear resistant composite. Am J Dent 1993;6(2):85–7.
[5] Boaro LC, et al. Correlation between polymerization stress and interfacial integrity of composites restorations assessed by different in vitro tests. Dent Mater 2014;30(9):984–92.
[6] Zhao IS, et al., Prevention of secondary caries using silver diamine fluoride treatment and casein phosphopeptide-amorphous calcium phosphate modified glass-ionomer cement. (1879-176X (Electronic)).
[7] Cheng L, et al., One-year water-ageing of calcium phosphate composite containing nano-silver and quaternary ammonium to inhibit biofilms. (2049-3169 (Electronic)).
[8] Zhang Y, et al. Quaternary ammonium compounds in dental restorative materials. Dent Mater J 2018;37(2):183–91.
[9] Cherchali FZ, et al. Effectiveness of the DHMAI monomer in the development of an antibacterial dental composite. Dent Mater 2017;33(12):1381–91.
[10] Cheng L, et al. Nanotechnology strategies for antibacterial and remineralizing composites and adhesives to tackle dental caries. Nanomedicine (Lond) 2015;10(4):627–41.
[11] Zhang N, et al. Current Insights into the modulation of oral bacterial degradation of dental polymeric restorative materials. Materials (Basel) 2017;10(5).
[12] Wu Y, et al. Long-term and controlled release of chlorhexidine-copper(II) from organically modified montmorillonite (OMMT) nanocomposites. Mater Sci Eng C Mater Biol Appl 2013;33(2):752–7.
[13] Hidalgo E, Dominguez C. Mechanisms underlying chlorhexidine-induced cytotoxicity. Toxicol In Vitro 2001;15(4–5):271–6.
[14] Liu JX, et al. Cytotoxicity evaluation of chlorhexidine gluconate on human fibroblasts, myoblasts, and osteoblasts. J Bone Jt Infect 2018;3(4):165–72.
[15] He HP, et al. A novel organoclay with antibacterial activity prepared from montmorillonite and chlorhexidini acetas. J Colloid Interface Sci 2006;297(1):235–43.
[16] Wang XY, Du YM, Luo JW. Biopolymer/montmorillonite nanocomposite: preparation, drug-controlled release property and cytotoxicity. Nanotechnology 2008;19(6).
[17] Wu Y, et al. Long-term and controlled release of chlorhexidine-copper(II) from organically modified. montmorillonite (OMMT) nanocomposites. Mater Sci Eng C 2013;33(2):752–7.
[18] Campos L, et al. DH and ESPI laser interferometry applied to the restoration shrinkage assessment. Radiat Phys Chem 2014;94(1):190–3.
[19] Munhoz T, et al. Effect of nanoclay addition on physical, chemical, optical and biological properties of experimental dental resin composites. Dent Mater 2017;33(3):271–9.
[20] Ambrogi V, et al. Montmorillonite-chitosan-chlorhexidine composite films with antibiofilm activity and improved cytotoxicity for wound dressing. J Colloid Interface Sci 2017;491:265–72.
[21] Cullity BD. Elements of X-ray diffraction. 2nd ed. Phillippines: Addison-Wesley Publishing Company Inc.; 1978.
[22] Stansbury JW, Dickens SH. Determination of double bond conversion in dental resins by near infrared spectroscopy. Dent Mater 2001;17(1):71–9.
[23] Muench A, et al. The effect of specimen dimensions on the flexural strength of a composite resin. J Appl Oral Sci 2005;13(3):265–8.
[24] Wayne P. Performance standards for antimicrobial disk susceptibility tests. Approved standard. 8th ed. CLSI; 2003. CLSI document M2-A8.
[25] Duarte S, et al. The influence of a novel propolis on mutans streptococci biofilms and caries development in rats. Arch Oral Biol 2006;51(1):15–22.
[26] Cogo K, et al. In vitro evaluation of the effect of nicotine, cotinine, and caffeine on oral microorganisms. Can J Microbiol 2008;54(6):501–8.
[27] da Cunha MG, et al. Antimicrobial and antiproliferative activities of stingless bee Melipona scutellaris geopropolis. BMC Complement Altern Med 2013;13:23.
[28] Fong N, Simmons A, Poole-Warren LA. Antibacterial polyurethane nanocomposites using chlorhexidine diacetate as an organic modifier. Acta Biomater 2010;6(7):2554–61.
[29] Sánchez-Valdes S, et al. Effect of PEgMA/amine silane compatibilizer on clay dispersion of polyethylene-clay nanocomposites. Polym Bull 2009;63(6):921.

[30] Barbosa AM, et al. Cellulose nanocrystal membranes as excipients for drug delivery systems. Materials (Basel) 2016;9(12).
[31] Luo D, et al. Synthesis of novel chlorhexidine spheres with controlled release from a UDMA-HEMA resin using ultrasound. Dent Mater 2017;33(6):713–22.
[32] Jeon HS, et al. Chlorhexidine-releasing orthodontic elastomerics. Dent Mater J 2015;34(3):321–6.
[33] Seneviratne CJ, et al. Nanoparticle-encapsulated chlorhexidine against oral bacterial biofilms. PLoS One 2014;9(8), e103234.
[34] Davies BM, Patel HC. Systematic review and meta-analysis of preoperative antisepsis with combination chlorhexidine and povidone-iodine. Surg J (N Y) 2016;2(3):e70–7.
[35] Sideridou I, Tserki V, Papanastasiou G. Study of water sorption, solubility and modulus of elasticity of light-cured dimethacrylate-based dental resins. Biomaterials 2003;24(4):655–65.
[36] Schweikl H, et al. Cytotoxic and mutagenic effects of dental composite materials. Biomaterials 2005;26(14):1713–9.
[37] Firestone AR. Effect of increasing contact time of sucrose solution of powdered sucrose on plaque pH in vivo. J Dent Res 1982;61(11):1243–4.
[38] Marsh PD. Plaque as a biofilm: pharmacological principles of drug delivery and action in the sub- and sup-ragingival environment. Oral Dis 2003;1(Suppl. 9):16–22.
[39] Paes Leme AF, et al. The role of sucrose in cariogenic dental biofilm formation–new insight. J Dent Res 2006;85(10):878–87.
[40] Casarin RC, et al. Levels of aggregatibacter actinomycetemcomitans, porphyromonas gingivalis, inflammatory cytokines and species-specific immunoglobulin G in generalized aggressive and chronic periodontitis. J Periodontal Res 2010;45(5):635–42.
[41] Bostanci N, Belibasakis GN. Porphyromonas gingivalis: an invasive and evasive opportunistic oral pathogen. FEMS Microbiol Lett 2012;333(1):1–9.
[42] How KY, Song KP, Chan KG. Porphyromonas gingivalis: an overview of periodontopathic pathogen below the gum line. Front Microbiol 2016;7:53.
[43] Lafaurie GI, et al. Microbiome and microbial biofilm profiles of peri-implantitis: a systematic review. J Periodontol 2017;88(10):1066–89.
[44] Cheng L, Weir MD, Zhang K, Arola DD, Zhou X, Xu HH. Dental primer and adhesive containing a new antibacterial quaternary ammonium monomer dimethylaminododecyl methacrylate. J Dent 2013;41(4):345–55, http://dx.doi.org/10.1016/j.jdent.2013.01.004.
[45] Murata H, Koepsel RR, Matyjaszewski K, Russell AJ. Permanent, non-leaching antibacterial surface–2: how high density cationic surfaces kill bacterial cells. Biomaterials 2007;28(32):4870–9.
[46] Tiller JC, Liao CJ, Lewis K, Klibanov AM. Designing surfaces that kill bacteria on contact. Proc Natl Acad Sci U S A 2001;98(11):5981–5.
[47] Alexandre M, Dubois P. Polymer-layered silicate nanocomposites: preparation, properties and uses of a new class of materials. Mater Sci Eng. R: Rep 2000;28(1):1–63.
[48] Beyth N, et al. Antibacterial activity of dental composites containing quaternary ammonium polyethylenimine nanoparticles against *Streptococcus mutans*. Biomaterials 2006;27(21):3995–4002.
[49] Sothornvit R, Rhim J-W, Hong S-I. Effect of nano-clay type on the physical and antimicrobial properties of whey protein isolate/clay composite films. J Food Eng 2009;91(3):468–73.
[50] Rhim JW, et al. Preparation and characterization of chitosan-based nanocomposite films with antimicrobial activity. J Agric Food Chem 2006;54(16):5814–22.